

Research on Structural Red Clay under Different Stress Conditions

Zhenyu Li^{1*}, Hongbin Xiao¹, Guolin Yang², Yonghe Wang²

^{1*}Corresponding author, School of Civil Engineering and Mechanics, Central South University of Forestry and Technology, Changsha 410004, China ; hdlizhenyu@163.com

²Director, School of Civil Architectural Engineering, Central South University, Changsha, 410075, China, guoling@mail.csu.edu.cn

ABSTRACT: Red clay is a typical particular soil in China, whose particular engineering properties are concerned in the engineering. Based on the laboratory test results of undisturbed samples from different depths, physico-mechanical properties of structural red clay can be investigated. Structural character of soil is analyzed combining the plat load test. It is investigated that there are three factors effecting on the structure of red clay. The results are presented for different drained triaxial tests on different depth soils specimens under different consolidated stress states. Simulating the process of stress changes and stress states, some conclusions of mechanic properties of red clay under different stress level can be drawn. It is discussed that some factors influence the strength and deformation of structural red clay, such as structure, stress level, stress paths and so on.

Key words: red clay; structure; stress level; strength

INTRODUCTION

Red clay is a high plastic clay body which comes from carbonate rocks in tropical and subtropical humid climatic conditions under the action of the physical or chemical weathering. It is brownish red and reddish brown in color. The physical and chemical characteristics of red clay are different with common clay. Furthermore, the variation regulars of these characteristics along depth of soil body are contrary with other clay soil, which appears significant difference. These are attributed to red clay's constituents, structure and it's the very complex interaction, particularly structure. The paper discusses the deformation and mechanical characteristics of red clay through many tests on it. The soil samples are taken out from the construction site of a passenger dedicated line. Many experiments have been carried out such as triaxial tests of different consolidation and drainage conditions on different depths soil samples. Through these tests, strength properties and deformation characteristics of structural red clay have been discussed under different stresses.

BASIC PHYSICAL AND MECHANICAL PROPERTIES

The accuracy of laboratory test results is affected by many factors, such as excavating soil, handling, soil preparation, operation technology, test equipment and so on. To ensure the quality of soil, some measures have been taken to keep soil sample specimen and the original structure of the natural moisture, including using appropriate drilling equipment and technology, strictly dug operating procedures. In addition, single-action triple the soil management has been used to take out soil samples, which can disturb less on soil. In the process of laboratory tests for soil index measurements, the error caused by human and the instrument itself can be reduced by strict operation according to experimental rules. Laboratory test results are obtained as following table 1.

Table 1. Physical indexes of red clay

No.	Soil depth H(m)	Water content w(%)	Density ρ (g/cm ³)	Void ratio e	Liquid limit W _L (%)	Plastic Limit W _p (%)	Plastic Index I _p
1	0.9	25.00	2.01	0.70	51.10	29.90	21.20
2	2.6	25.90	2.02	0.70	54.80	24.30	30.60
3	3.9	25.59	2.02	0.70	57.50	30.00	27.60
4	4.8	27.69	1.99	0.76	65.90	25.90	40.00
5	5.2	37.69	2.04	0.72	65.90	25.90	40.00
6	9.9	39.97	1.85	0.92	66.90	34.70	32.20
7	10.5	43.97	1.87	0.90	66.90	34.70	32.20
8	11.1	48.60	1.92	0.80	61.90	28.00	33.90
9	12.7	62.59	1.78	1.02	73.90	34.20	39.80

Table 2. Deformation indexes of red clay

Compression index C_c	Compression modulus E_s (Mpa)	Deformation Modulus E_0 (Mpa)	Expansion index C_s (10 ⁻²)	Volume contraction rate δ_v (% ²)	free swelling ratio δ_{ef} (%)	Expansion ratio with no load δ_e (%)	Expansion ratio with load δ_{ep} (%)	Contraction Coefficient λ_s
0.06~0.26	12.8~37.5	9.0~31.1	0.7~1.2	10.3~13.7	0.06~0.26	0.99~1.77	-1.58~-0.82	0.22~0.52

From table 1, some indexes of red clay such as water content, void ratio and specific gravity are significantly higher than other clay's. In the vertical profile of red clay body, with the increasing of soil depth, soil water content increases and density decreases. High liquid limit and plastic limit, but liquid index is lower. From top to down soil layer, red clay are respect the hard plastic soil, plastic and soft plastic state. The results can be drawn from Table 2 that the performance of mechanical properties of red clay soil appears low compression. For this red clay with some characteristics of water content, high void ratio, low compression, dehydration shrinkage significantly, it can be analyzed from microscopic aspect. The main minerals in red clay are flaking mineral.

Under high temperature and humidity conditions in the tropical-subtropical region, red clay have formed a unique structure of free iron oxide in the cement through complex laterization process. There is very strong cohesive force within pellets of clay minerals. Many porous become snort porous when external force is not big. Thus a high-porosity characteristic appears in soil structure. But the high structural strength within the aggregate comes from the free oxides cementation in soil internal structure.

TRIAXIAL TEST RESEARCH OF RED CLAY

Soil samples preparation

Structured red clay soil was inhomogeneous soil. It has been found by drilling survey on-site the state of soil can be changed from hard plastic to plastic, then to soft plastic from the upper to the lower soil layer. That is to say, there exist all consistency states in red clay soil body from up to lower layer. To understand all the mechanical properties of red clay soil under load, different depths of soil samples have been tested. Considering the different combinations of axial stress and confining pressure in different consolidated state and shear phase, the project has carried out a series of static triaxial tests on different depths soil samples under four stress levels and three drainage conditions simulating the actual stress state of soil.

Stress and strain relation

Some isotropic consolidation shear tests and triaxial shear tests have been carried out. The relationship between deviator stress $\sigma_1 - \sigma_3$ and axial strain has been showed as figures. The figure 1 shows the curves of deviator stress and axial stress. It has showed there appears strain hardening phenomena at different degree at the same depth, confining pressure, shear rate and different drainage conditions. The hardening phenomenon is more significant on the consolidation of drainage. But it does not appear hardening phenomenon on the consolidation of undrainage. The original shear modulus obtained by consolidated drainage tests is bigger than those obtained by unconsolidated drainage tests.

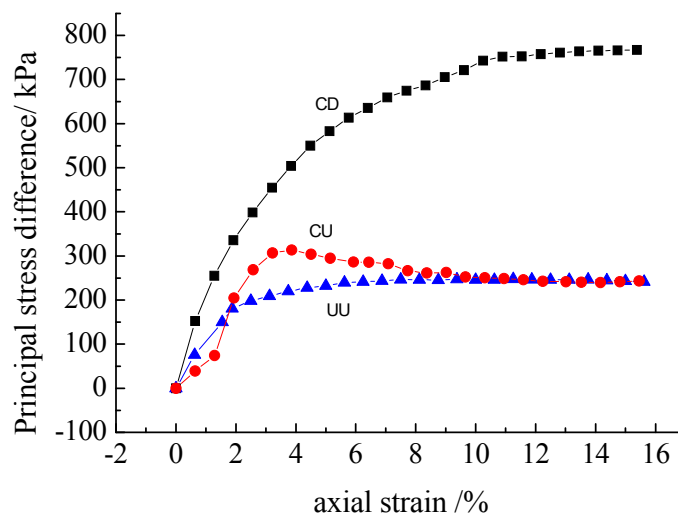


FIG. 1. Relations of deviatoric stress and axial-strain

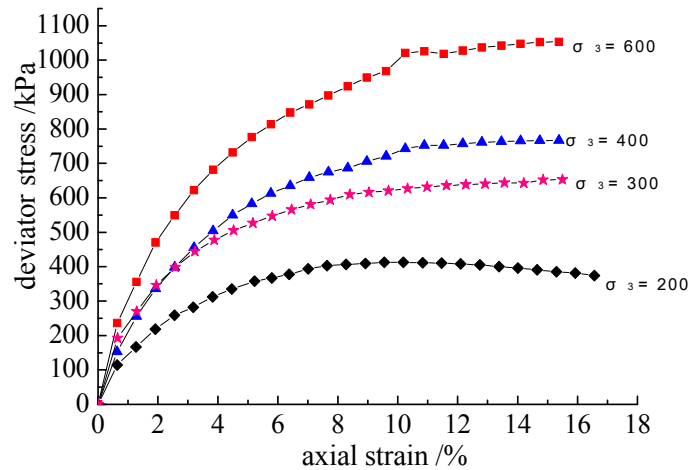


FIG.2. Relations of deviator stress and axial-strain

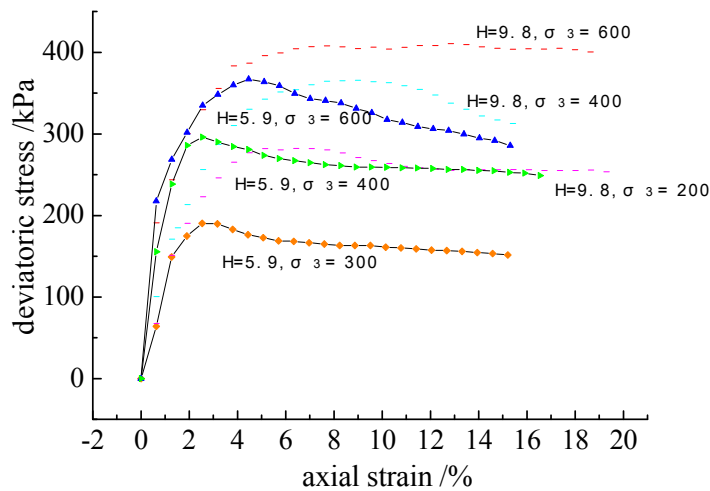


FIG.3. Relations of deviator stress and axial-strain

Figure 2 shows the relation of deviator stress and axial strain by consolidated drainage tests under the condition of the same depth and different confining pressure. These curves have no peak and appear hardening trend. The curves have showed under the same axial stress soil samples with smaller confining pressure appear the greater the deformation. And these soils occur yielded first. These phenomena illustrate the soil with high confining pressure can resist deformation strongly and their deviator stresses are much big when they occur yield. It agrees with the results of common clay by triaxial tests.

Figure 3 shows the relation of deviator stress and axial strain by consolidated drainage tests on soil samples from two different depths layer. The solid line is result of 5.9m soil sample. The dotted line is result of 9.8m soil sample. It can be seen from the chart that the properties of two sites soil are significantly different. The curves of stress and strain of 5.9m depth soil sample are softening curves in which the values of stress will

increase to a peak with strain of soil increasing, and then decrease with soil' strain continue increasing. However, the curves of stress and strain of 9.8m depth soil sample are hardening curves in which the values of stress will increase with strain of soil increasing, but the increasing rate become more and more slow.

It can be draw from above that the shallow soil is over consolidation clay and the deep soil is normally consolidated clay. And over consolidation rate of red clay decreases with depth increasing. This characteristic of consolidation is contrary to that of common clay. This phenomenon demonstrates red clay has the property of strong structural, which play an important role to some other engineering characteristic, such as high void ratio, low-compression and so on. There are many factors effecting strong structural of red clay. At present, more and more researchers believe the main factor is the internal colloidal structure of red clay produced by oxide in soil through chemical reaction. The literature had analyzed chemical composition of red clay from upper to deep soil layer and obtained that iron oxide content decreased with soil depth increasing. Therefore, deep layer red clay is plastic, even soft plastic state. The key lies on the reduction of oxide in deep soil layer.

Shear strength of red clay

The main strength parameters of clay are the cohesion and friction angle which reflect the characteristics of soil particles and micro-structure coupling of soil. Usually the shear strength of clay will increase with the normal stress or confining pressure increasing. From figure 2 and figure 3, the deformation modulus of red clay increase with confining pressure increasing because there is constrained force provided by confining pressure, which is important to strength and stiffness of soil. This is one important characteristic different from other materials.

Table 3. Strength of red clay

c_{cd} (kPa)	φ_{cd} (°)	c_u (kPa)	φ_u (°)	c_{cu} (kPa)	φ_{cu} (°)
11.5~60.8	9.9~29.6	18.9~67	5.7~26.9	11.6~69.7	8.1~26.4

Table 3 is the strength of soil obtained by triaxial tests under the different consolidated stress and drainage conditions.

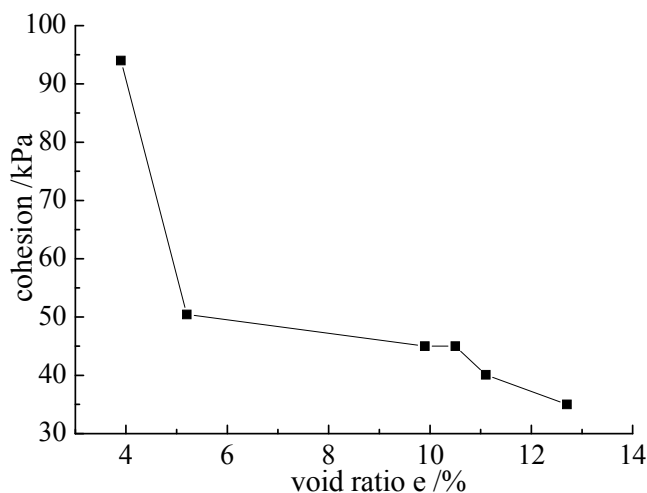


FIG.4. Relation of cohesion and void ratio

Figure 4 shows cohesion increase with void ratio increasing. The void ratio of red clay increases with soil depth increasing, which is different from other clay. The value of cohesion is much bigger, the stronger structure link between the soils particles. If soil particles are coarse and the density of soil is low, then the value of friction angle is big and the friction between soil particles is the greater. This agrees with the physical and mechanical properties of soil obtained by laboratory tests. Due to evaporation effects, the water contents of surface soil decrease. The soil on surface will shrink and then harden. Consequently, surface soil is usually in hard plastic or hard state and the soil is much soft with depth increasing. On another aspect, evaporation effects intensify the aging process of free oxides of dehydration in soil body. It makes more free oxide colloidal crystallization precipitate, which can enhance soil structure connection and strengthen the mechanical strength of soil.

CONCLUSIONS

The consolidation of different depth soil in natural state will be different under the action of weight. Even if soil is consolidated at the same stress, the density and structure of soil with different water content will be different. In addition, the changes of water content will effect on the arrangement and structure of soil particles.

Based on a lot of conventional tests and triaxial shear tests by different methods on different depth soil samples, it has obtained the relations of stress and strain of red clay under different consolidations and drainage conditions. Different depths soil has different characteristics of hardening and softening. The results of experiments have showed physical and mechanical properties of structured red clay are spatial. They will change with soil depth increasing in regular.

ACKNOWLEDGMENTS

The authors appreciate the support of National Natural Science Foundation of China (No.50978097).

REFERENCES

- Li Guangxin(2003). "Advance soil mechanic. " Beijin: *Tsinghua University Press*:51-56
- Jiang Mingjin, Shen Zhujiang, Xing Shuyin(1999). "Review on Structured Clay. " *ADVANCES IN SCIENCE AND TECHNOLOGY OF WATER RESOURCES*, Vol.19(1):26-31
- Huang Zhihong, Zhu Lijun, Liao Yilin(2004). "MECHANICAL PROPERTIES OF RED CLAY UNDER DIFFERENT STRESS PATHS. " *CHINESE JOURNAL OF ROCK MECHANICS AND ENGINEERING*, Vol.23(15):2599-2603
- Tan Luorong, Kong linwei(2001). "Fundamental property and microstructure model of red clay. " *CHINESE JOURNAL OF GEOTECHNICAL ENGINEERING*, Vol.23(4):458-462

- Zhao Yinwen, Kong Linwei, Guo Aiguo(2004). "COMPARATIVE LABORATORY STUDY ON TYPICAL RED CLAY AND EXPANSIVE SOIL. " *CHINESE JOURNAL OF ROCK MECHANICS AND ENGINEERING*, Vol.23(15) : 2593-2598
- Liu Enlong, Shen Zhujiang(2006). "MECHANICAL BEHAVIOR OF STRUCTURED SOILS UNDER DIFFERENT STRESS PATHS. " *CHINESE JOURNAL OF ROCK MECHANICS AND ENGINEERING*, Vol.25(10):2058-2065
- Zhou Xunhua, Liao Yilin(2004). "Collochemistry Character of the Structure Connection Among Red Clay Mineral Grain. " *JOURNAL OF GUIZHOU UNIVERSITY OF TECHNOLOGY (NATURAL SCIENCE EDITION)* , Vol.33(1):26-29
- Davis E H, Raymond G P(1965). "A nonlinear theory of consolidation. " *Geotechnique*, Vol.15(2): 161-173
- Tang Liansheng, Wang Yang, Zhang Pengcheng(2003). "Experimental study on suctions between grains in unsaturated cohesive soil. " *CHINESE JOURNAL OF GEOTECHNICAL ENGINEERING*, Vol.25(3):304-307

UTILIZING GROUND PENETRATING RADAR FOR ROADWAY STRUCTURE INSPECTIONS

Dar-Hao Chen¹ and Jeffrey L. Lee²

¹ Professor, Changsha University of Science and Technology. Chiling Road 45#, Changsha, Hunan, P.R.China, 410076 and Texas Department of Transportation, 4203 Bull Creek #39, Austin, TX 78731. darhao2008@gmail.com

² Senior Engineer – Pavements, AECOM, 540 Wickham Street, Fortitude Valley, QLD 4006, Australia. E-mail: Jeffrey.Lee@aecom.com

ABSTRACT

The nondestructive mapping of anomalies and voids under roadway pavements is critical to highway authorities because of the potential safety hazards caused by the loss of support. A 400 MHz Ground Coupled Penetrating Radar (GCPR) was utilized in this study to characterize subsurface voids. To enhance the understanding of the data collection and interpretation, different thicknesses of calibration concrete slabs with different depths of voids were designed and constructed. In addition, a field study using the GCPR was also conducted on US-290 with visible settlement. The extents of the anomalies in the horizontal and vertical directions were accurately identified from the GCPR images. Coring was performed to verify the extent of the subsurface void conditions. Fortunately, the voids near the drainpipes were detected by GCPR in time. Otherwise, the void would have been progressed in size, and that could have led to a severe hazard to the general public. This study has successfully demonstrated that the GCPR is able to identify anomalies and voids. Engineers can utilize the information from GCPR to undertake remedial actions with confidence.

INTRODUCTION

The transportation infrastructure around the world requires enormous resources for maintenance and upkeep. Detecting hidden subsurface voids under a pavement is critical to pavement asset management. The development of voids beneath roadways is a serious hazard, making early detection an important aspect of infrastructure maintenance and remediation. Leaks and breaking pipe allow fine aggregate to be carried away, resulting in local base erosion and pumping. This eventually leads to the formation of weak areas, and forming voids. The subsurface voids generally increase in size with time due to additional erosion and washout. In modern roadway engineering, one of the most useful and nonintrusive methods is the Ground Penetrating Radar

(GPR), which transmits and records the travel times of electromagnetic waves through the pavement layer structure. The GPR operates by transmitting an electromagnetic pulse from an antenna into the ground and then records the properties of the reflections of this pulse. Information such as the time taken for the reflected signals to return to the antenna and the amplitude and phase of the reflected signal were used to identify pavement layers and anomalies [Chen and Scullion 2008]. The reflected time record from the electromagnetic wave contains a record of the properties and thickness of the layers within the roadway structure. GPR technology is very effective for identifying areas where physical properties have changed, which may indicate potentially hazardous voids [Lesto and Hatcher 2002; Chen and Wimsatt 2010]. The time delay and the amplitude of reflected signals have been utilized by engineers [Hunaidi and Giamou 1998, Loken 2007, Chen and Wimsatt 2010] to characterize the subsurface pavement conditions. Objects or areas that have different electrical properties (or dielectric constants) will reflect the pulse differently, and appear as anomalies.

In general, air voids and water-filled voids are both detectable by GPR, because the impedance between the dielectric constants of both air (1.0) and water (81) are substantially different than most pavement materials. If the void is air-filled, a large negative peak will appear in the waveform, since the dielectric constant of air is much less than pavement material. Conversely, a large positive peak in the waveform will appear at the surface of a water-filled void, because the dielectric increases substantially at the interface.

This paper presents two case studies utilizing a 400 MHz Ground Coupled Penetrating Radar (GCPR) to identify subsurface voids. The GCPR surveys were performed at walking speed (approximately 5km/hr). The first case study was conducted on the calibration slabs that have known prefabricated voids. The second case study was performed on US-290, which has visible settlement and a fair probability of hidden voids under the pavement structure.

CALIBRATION SLABS

Calibration slabs with three different slab thicknesses and different depths of voids, were constructed at the Texas Tech University campus. Void at 30, 18, 6 and 3 inches (762, 457, 152, and 76mm) depth from the surface were constructed within the slabs, as shown in Fig. 1. The voids were rectangular, 8ft (2.44m) long by 2ft (0.61m) wide. All air voids were created with wooden formworks.

Slabs were also constructed with a range of slab thicknesses: (1) 15 inches (2) 11 inches, and (3) 8 inches. Each slab was constructed with the dimensions of 15ft by 12ft (4.57m by 3.66m). For comparison purposes, one slab without voids was built 8 inches (203mm) thick. Since the majority of the voids found in Texas are under continuously reinforced concrete pavement (CRCP), the calibration slabs were built with CRCP. The 15-inch (381mm) slab is constructed with two layers of steel. All other slabs were constructed with one layer of steel. TxDOT's specifications require two layers of steel when a CRCP is 14 inches (356mm) or thicker. Fig. 1 illustrates the slab and void dimensions as well as steel reinforcements layout.

GCPR surveys were conducted on a grid pattern, both longitudinal and transverse directions. The GPR results for 8-inch (203mm) slabs are shown in Fig. 2. In the upper left corner, the numbers 30, 32, 34, to 54 denote the GPR runs. Anomalies due to voids are clearly shown in GPR traces, as presented in Fig. 2.

Trace numbers 33 and 39 in Fig. 2 correspond to GPR tests at the center of the 30 and 6 inch (762 and 152 mm) deep voids, respectively. Trace number 53 is superimposed in Fig. 2 to compare the slab with void to the no-void condition. In view of Fig. 2, large negative peaks appeared in the waveforms for tests 33 and 39, indicating that the voids are air-filled. There are no voids for the first two feet, thus no large negative peaks appeared in the waveforms for tests 33 and 39, until the void was encountered. No evidence of a large negative peak on test 53 can be identified, because there was no void built into tract 53.

To verify the void thickness, Eq. 1 is employed.

$$H_a = \frac{c \cdot \Delta t_1}{2\sqrt{\epsilon_a}} \quad [1]$$

where

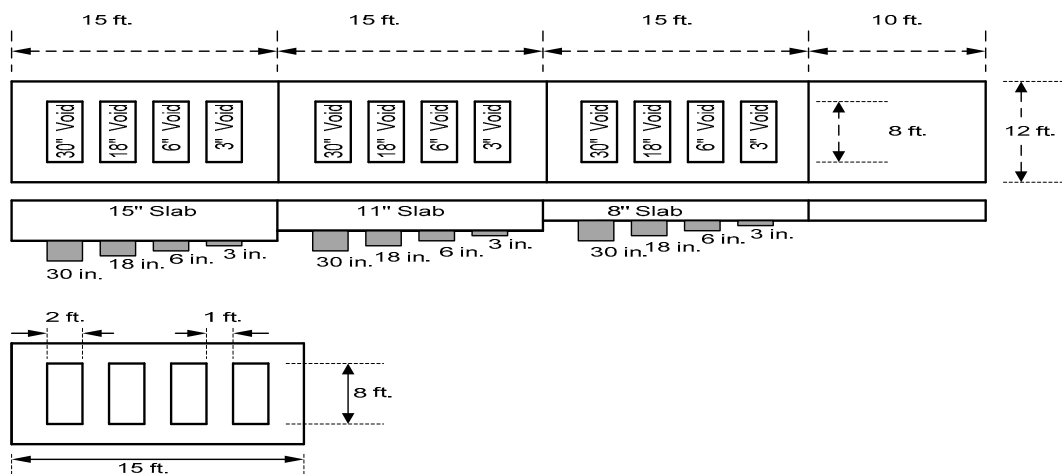
H_a = thickness

c = a constant (speed of light in air=.30 m/ns)

ϵ_a is the dielectric constant of the pavement layer

Δt_1 = The time interval between peaks which represents the two-way travel time through the pavement layer. Ranges of dielectric constants for typical pavement materials are given in Table 1.

The large negative peaks in Fig. 2 indicate the beginning of the void. Based on Eq. 1 and the constructed void thickness information, the starting and ending position of the void is labeled in Fig. 2.



Wood boxes that filled with air voids